

Fabrication of Cu₂O/Fe-O heterojunction solar cells by electrodeposition

J. J. M. Vequizo², C. Zhang¹, and M. Ichimura¹

¹ Department of Engineering Physics, Electronics and Mechanics, Nagoya Institute of Technology, Nagoya, 466-8555, Japan

² Graduate School of Engineering, Toyota Technological Institute, 2-12-1 Hisakata, Tempaku, Nagoya 468-8511, Japan

Abstract

Cu₂O/Fe-O heterojunction solar cells were successfully fabricated by electrodeposition method. The as-deposited thin film exhibited signature Raman peaks associated to γ -FeOOH. By thermal annealing in air at 100 – 400°C, different Fe₂O₃ polymorphs were produced. Both as-deposited and annealed Fe-O films showed *n*-type conductivity with approximated band gap of 2.1 - 2.3 eV. Resistivity was ~680 Ω cm for γ -FeOOH and > 700 Ω cm for Fe₂O₃ films. Cu₂O as the *p*-type layer was partnered with as-deposited and annealed Fe-O thin films to fabricate different heterojunctions based on Fe oxides compounds. Remarkably, all the fabricated Cu₂O/Fe-O heterostructures exhibited photovoltaic characteristics (open circuit voltage, $V_{OC} = 38$ -108 mV and short circuit current density, $J_{SC} = 0.74 - 1.58$ mA/cm²), although no appreciable differences were found on their solar cell parameters. The present results strongly suggest the potential of Fe-O based semiconductors for solar cell fabrication.

Keywords

electrodeposition, heterojunction, γ -FeOOH, Fe₂O₃, Cu₂O

1. Introduction

Iron oxide (Fe_2O_3) has been studied for application of photoanodes owing to their semiconducting characteristics, abundance in the earth crust, and environmental compatibility. Fe_2O_3 is an *n*-type semiconductor with a band gap $E_g = 2.0 - 2.2$ eV, and the photoanodes based on it is capable to utilize approximately 40% of the incident sunlight [1]. It has been reported that iron oxyhydroxide ($\gamma\text{-FeOOH}$), also an *n*-type semiconductor with a band gap > 2.0 eV, is potentially useful for solar energy conversion [2]. However, those Fe-O phases have not been applied for *p-n* heterojunction solar cells, although they have been studied as photocatalysts quite extensively. Recently, our research group successfully fabricated $\text{Cu}_2\text{O}/\gamma\text{-FeOOH}$ *p-n* junction and confirmed the photovoltaic properties [3]. From these results, we are convinced that the Fe-O phases can be novel candidates for *n*-type window (or buffer) layer materials of heterostructure solar cells. However, as far as we know, the fabrication of *p-n* junctions based on Fe_2O_3 has not been tried yet. It is known that $\gamma\text{-Fe}_2\text{O}_3$ (cubic, spinel structure) and $\alpha\text{-Fe}_2\text{O}_3$ (rhombohedral, corundum structure) can be produced by annealing the iron oxide hydroxides ($\gamma\text{-FeOOH}$) at a suitable temperature [4-7]. The resistivity of $\alpha\text{-Fe}_2\text{O}_3$ was reported to be rather high (about 10^4 Ωcm) at room temperature [8].

In this study, $\gamma\text{-FeOOH}$ films are deposited using electrodeposition (ED) and subsequently annealed in air at $100 - 400^\circ\text{C}$ to produce Fe_2O_3 phases. As in the previous work [3], Cu_2O is utilized as a *p*-type semiconductor material to fabricate *p-n* heterojunction solar cells with the Fe-O layer as the *n*-type layer, and the photovoltaic properties of $\text{Cu}_2\text{O}/\text{Fe-O}$ heterojunction are evaluated and investigated. Cu_2O has been widely studied as a typical *p*-type semiconductor material (with direct band gap, $E_g = 2.0 - 2.1$ eV) in heterojunction solar cells partnered with a lot of other semiconductors, such as SnO_2 , CdO [9], Ga_2O_3 [10], and ZnO [11-14]. In contrast to heterostructures based on Cu_xS , any serious problems due to Cu diffusion have not been reported for those heterostructures based on Cu_2O . In this work, Cu_2O is also deposited using ED. ED is a simple chemical technique, by which a thin film can be deposited in a large area at a low cost, and thus it is advantageous for solar cell production. The results suggest that the heterostructures based on the as-deposited and annealed Fe-O films show photovoltaic properties, and therefore, both Fe_2O_3 and FeOOH can be hetero-partners for other *p*-type absorbers.

2. Experimental details

γ -FeOOH thin films were potentiostatically electrodeposited onto indium tin oxide (ITO)-coated glass substrate using the three electrode electrochemical cell with platinum sheet and saturated calomel electrode (SCE) as counter and reference electrodes, respectively [2]. An aqueous solution containing 50 mM $\text{FeSO}_4 \cdot 7\text{H}_2\text{O}$ and 100 mM Na_2SO_4 was prepared for ED. Subsequently, the as-prepared solutions were saturated with oxygen by bubbling before the deposition started; the bubbling rate was kept at 0.5 L/min. The γ -FeOOH films were deposited on the $1 \times 1 \text{ cm}^2$ exposed area of the ITO electrode by applying a constant cathodic potential of -0.9 V vs SCE. The experiment was carried out using freshly prepared solution for each deposition to ensure that the reaction is mainly due to electroreduction of Fe^{2+} , water, and dissolved oxygen producing FeOOH film. As already reported in our previous work, possible hydrolysis of Fe^{2+} , forming yellowish colloidal precipitates, occurred when the deposition and oxygen bubbling duration were extended [2]. All the depositions were carried out at room temperature and in a stirred solution for 10 min. The deposited γ -FeOOH thin films with a thickness about 300 ~ 500 nm were annealed at 100, 200, 300, and 400°C for 1 h in ambient air using the tube furnace. To fabricate $\text{Cu}_2\text{O}/\text{Fe}-\text{O}$ heterojunctions, the Cu_2O layer was then galvanostatically electrodeposited onto the as-prepared and annealed Fe-O films from the solution containing 0.2 M CuSO_4 and 1.6 M $\text{C}_3\text{H}_6\text{O}_3$ (with pH adjusted to 12.5 using KOH) with a constant cathodic current density of $-1.0 \text{ mA}/\text{cm}^2$ at solution temperature of 40°C [13,14]. The deposition duration for the Cu_2O layer was maintained for 10 min. We did not find significant dissolution of the Fe-O layers in the Cu_2O deposition solution. In fact, Fe-O is known to be stable in alkaline solutions (an Fe-O anode usually works in a 1 M NaOH solution in the photocatalyst application [1]).

A JASCO U-570 ultraviolet/visible/near infrared spectrometer was utilized for optical transmission studies with the ITO substrate as the reference. The thickness of the films was measured with an Accretch Surfcom-1400D profilometer. Compositional analysis was carried out by using a JEOL JAMP-9500F field-emission Auger electron spectroscopy (AES). Argon ion etching was performed to sputter the film's surface at an acceleration voltage of 2 kV and ion current of 2.6 mA. AES spectra were recorded after 30 s of sputtering at a rate of 10 nm/min. The composition ratio (Fe/O) was calculated using standard Fe_2O_3 compound as a reference material. Raman spectroscopy was done by applying a JASCO NRS-3300 laser Raman spectrophotometer. A red laser with 632.83 nm wavelength was utilized in Raman spectroscopy.

To determine the conductivity type and photoresponse, photoelectrochemical (PEC) measurement was performed by utilizing the three-electrode electrochemical cell with aqueous 0.1 M Na₂SO₄ as the electrolyte. The voltage was scanned linearly towards the forward bias region, and the sample was illuminated from the substrate side to evaluate the photoresponse.

After the fabrication of Cu₂O/Fe-O heterojunction, indium electrodes with 1 mm² area each were evaporated on top of the heterostructure for electrical contacts. Thus, the structure of the solar cell is In/Cu₂O/Fe-O/ITO. Since the resistance along the film surface is expected to be much higher than that in the thickness direction, each electrode is considered to be effectively isolated. We confirmed that In is a good ohmic metal for both Cu₂O and Fe-O without any thermal treatment. The photovoltaic properties of the cell were evaluated by using a solar simulator under AM1.5 (100 mW/cm²) illumination condition. The heterostructure was exposed to the irradiation from the ITO substrate side.

3. Results and discussion

3.1 Compositional and morphological characterizations

The composition of the as-deposited and annealed films was obtained from the differential AES spectra shown in Figure 1. As seen in Figure 1(a), the Fe and O peaks are clearly observed with Fe/O ratio of approximately 0.52. Similar AES spectrum was observed for annealed films. The representative spectrum is shown in Figure 1(b) for the film annealed at 400°C. As indicated, the Fe/O ratio is approximately 0.67, which is very close to the stoichiometric ratio of Fe₂O₃. The estimated Fe/O ratios for other annealed samples are listed in Table 1. It is noted that the Fe/O ratio remains at around 0.5 when the annealing temperature is 100°C, and it increases to around 0.67 as the temperature \geq 200 °C. This appreciable change in Fe/O ratio indicates transformation of the as-deposited film to Fe₂O₃.

Raman spectroscopy was performed to further examine the phase transformation upon annealing. The Raman shifts of the as-deposited and annealed Fe-O thin films are shown in Figure 2. As seen in in Figure 2(a), the as-deposited film exhibited sharp peaks at 252 and 384 cm⁻¹ and broad peaks at 537 and 663 cm⁻¹, which are characteristic Raman shifts of γ -FeOOH in good agreement with the reported Raman peaks of γ -FeOOH in the literature [15-17]. Hence, these results confirmed the successful deposition of γ -FeOOH. For films annealed at 100 – 400°C, the Raman spectra depicted in Fig. 2(b) change as the temperature increases. At 100°C, the Raman peaks are very similar to that of the as-deposited film, implying that the

film is still γ -FeOOH. However, as the calcination temperature progresses from 200 – 300°C, the characteristic peaks associated to γ -FeOOH completely disappeared. The peak positions are now located at 345, 398, 486, 670, and 710 cm^{-1} , which agree very well with the reported Raman shifts of γ -Fe₂O₃ phase. Further annealing at 400°C resulted to Raman spectrum with obvious peaks at 221, 291, 407, 486, and 608 cm^{-1} , which are signature Raman shifts for α -Fe₂O₃ [15-17]. The above results suggest that γ -FeOOH transforms to γ -Fe₂O₃ at around 200°C and finally transforms to thermally stable α -Fe₂O₃ at around 400°C [4-7].

Figure 3 shows the SEM images of the films annealed at (a) 100, (b) 200, (c) 300, and (d) 400°C. The morphology of the annealed samples seems to be somewhat refined with increase in annealing temperature. The thickness of the as-deposited Fe-O film is about 400 nm. There is a thickness fluctuation (about 20%) within the deposition area. It is noted that no significant change in thickness was observed for annealed films, which suggests that the roughness of the films reduces by annealing while the thickness remains constant.

3.2 Optical transmission and photoelectrochemical measurements

Figure 4 shows the results of the optical transmission measurement for as-deposited and annealed Fe-O thin films. As seen, the absorption edge lies between 500 and 600 nm for as-deposited film. Interference patterns are not observed probably because of scattering due to surface roughness, and thus we did not consider the interference effects in the analyses. For band gap estimation, the Tauc's plot obtained using the transmission data for as-deposited γ -FeOOH is shown in the inset of Figure 4. By extrapolation of the linear region, the direct band gap is approximated to be 2.3 eV. The optical transmissions of Fe-O thin films under different annealing temperatures are indicated in the figure. As observed, the absorption edge for annealed Fe-O films is still between 500 – 600 nm, suggesting that no appreciable change in the band gap is expected. The estimated band gap for films annealed at 200 - 300°C is 2.2 eV, which agrees well with the reported band gap obtained for γ -Fe₂O₃ nanowires [18]. The band gap of 400°C-annealed Fe-O film is slightly reduced to 2.1 eV, which is a typical value for α -Fe₂O₃ [1].

Figure 5 shows the PEC measurement of the as-deposited and 100°C-annealed γ -FeOOH. No photocurrent response is observed during negative bias, whereas the photocurrent response is clearly observed during positive bias. Because the photocurrent is positive, the photogenerated minority carriers are holes. This signifies *n*-type conductivity. The PEC response of the film annealed at 100°C also shows

positive photocurrent, indicating *n*-type conductivity. It is noted that all the annealed samples give similar *n*-type conductivity and photoresponse.

3.3 Photovoltaic characteristics of Cu₂O/Fe-O heterostructures

The current-voltage (J-V) characteristics of Cu₂O/ γ -FeOOH and Cu₂O/ α -Fe₂O₃ heterostructures are depicted in Figure 6. As can be seen, both the heterostructures demonstrate rectification properties and the current density increases upon illumination. Furthermore, all the fabricated heterojunctions with Fe-O thin films annealed at different calcination temperatures exhibit photovoltaic characteristics as shown in Figure 7. The solar cell performance is listed in Table 2. Herein, we can see that the estimated solar cell parameters show no big difference. The solar conversion efficiency of the Cu₂O/Fe-O heterojunction is low (< 0.1%), which could be partly due to high resistivity of the deposited layers. We evaluated the resistivity of γ -FeOOH, γ -Fe₂O₃ and α -Fe₂O₃ layers by comparing the J-V characteristics of the In/Fe-O/ITO structures with those of the In/ITO structure. The approximated resistivity of γ -FeOOH, γ -Fe₂O₃ and α -Fe₂O₃ layers is 680 Ω cm, 780 Ω cm, and 35 k Ω cm, respectively. The resistivity of Cu₂O is about 3 k Ω cm. The total thickness of the cell is rather small (about 1 μ m), but still the cell can absorb the light of wavelengths < 500 nm almost completely. Thus, the thickness is not the main reason for the low efficiency. The stability of the Cu₂O/Fe-O heterostructures was also examined under prolonged irradiation. It was observed that the V_{OC} for Cu₂O/FeOOH cell decreased by about 30%, whereas the I_{SC} remained almost the same after 6 h irradiation. For the Cu₂O/Fe₂O₃ junction, the decrease in V_{OC} was nearly 25%, but the J_{SC} did not decrease significantly. Furthermore, we found that the V_{OC} can be recovered when the Cu₂O/Fe-O junctions are allowed to cool down after a prolonged exposure to light, for instance, within 1-hour after the 6-h irradiation, the V_{OC} recovered to 80% of the initial value. Thus, it can be speculated that the decrease in V_{OC} is partly due to heating and partly due to degradation of the Cu₂O/Fe-O cells during the prolonged illumination.

In our previous work, it was found that γ -FeOOH is a suitable *n*-type material in a heterojunction solar cell. The results of the effect of annealing indicate that the γ -FeOOH phase remains even after the 100°C annealing and thus can be regarded as stable under the usual operating condition of a solar cell. By the annealing at temperatures higher than 200°C, γ -FeOOH transforms to γ -Fe₂O₃ and α -Fe₂O₃. All of the Fe-O phases have similar band gap and photosensitivity. The heterostructures consisting of those Fe-O phases and Cu₂O exhibited rectification and photovoltaic properties, and there is no obvious difference in

the solar cell performance between them. Those results signify that γ -FeOOH, γ -Fe₂O₃ and α -Fe₂O₃ can be applicable as an n-type material to fabricate *p-n* heterojunction solar cells.

4. Conclusion

Cu₂O/Fe-O heterojunctions were successfully fabricated by ED. γ -FeOOH films were electrodeposited from oxygen-saturated FeSO₄-Na₂SO₄ aqueous solutions, and γ -Fe₂O₃ and α -Fe₂O₃ layers were fabricated by annealing the γ -FeOOH films in ambient air. As-deposited and annealed Fe-O films showed *n*-type conductivity with approximated band gap of 2.1 - 2.3 eV. The Cu₂O/Fe-O heterostructures were fabricated by depositing Cu₂O on the as-deposited and annealed Fe-O films. It should be noted that all the fabricated Cu₂O/Fe-O heterostructures demonstrated photovoltaic properties with open circuit voltage (38 - 108 mV) and short circuit current density (0.74 – 1.58 mA/cm²), although no notable differences were obtained in the approximated solar cell parameters. These results clearly suggest that γ -FeOOH, γ -Fe₂O₃ and α -Fe₂O₃ can be utilized as *n*-type semiconductor in *p-n* heterojunction solar cells. To the best of our knowledge, these Cu₂O/ γ -Fe₂O₃ and Cu₂O/ α -Fe₂O₃ heterojunctions were fabricated for the first time, and hence the present findings introduce additional choices for *n*-type semiconductor to fabricate heterojunction solar cells.

Acknowledgements

The authors would like to thank Mr. Q. Tsukada for his technical assistance in AES measurement and Dr. M. Kato for his helpful suggestions.

References

- [1] K. Sivula, F. Le Formal, M. Grätzel, *Chem. Sus. Chem.* 4 (2011) 432 – 449
- [2] J. J. M. Vequizo, M. Ichimura, Electrodeposition and characterization of γ -FeOOH thin films from oxygen-bubbled aqueous iron sulfate solutions, *Appl. Phys. Express* 6 (2013) 125501.
- [3] J. J. M. Vequizo, M. Ichimura, Fabrication of $\text{Cu}_2\text{O}/\gamma$ -FeOOH heterojunction solar cells using electrodeposition, *Appl. Phys. Express* 7 (2014) 045501.
- [4] H. Naono, K. Nakai, Thermal decomposition of γ -FeOOH fine particles, *J. Coll. Interface Sci.*, 128 (1989) 146-156.
- [5] F. S. Yen, W. C. Chen, J. M. Yang, C. T. Hong, Crystallite size variations of nanosized Fe_2O_3 powders during γ - to α -phase transformation, *Nano Lett.* 2 (2002) 245-252.
- [6] R. Giovanoli, R. Brüttsch, Kinetics and mechanism of the dehydration of γ -FeOOH, *Thermochimica Acta*, 13 (1975) 15-36.
- [7] M. Macia, J. Morales, J.L. Tirado, C. Valera, Effect of crystallinity on the thermal evolution of γ - Fe_2O_3 , *Thermochimica Acta*, 133 (1988) 107-112.
- [8] S.K. Patapis, Electrical resistivity of α - Fe_2O_3 and comparison to TEP at the first order Morin transition, *Solid St. Commun.* 52 (1984) 925-928.
- [9] L. Papadimitriou, N. A. Economou, D. Trivish, Heterojunction solar cells on cuprous oxide, *Sol. Cells* 3 (1981) 73-80.
- [10] T. Minami, Y. Nishi, T. Miyata, High-efficiency Cu_2O -based heterojunction solar cells fabricated using a Ga_2O_3 thin film as n-type layer, *Appl. Phys. Express* 6 (2013) 044101.
- [11] A. Mittiga, E. Salza, F. Sarto, M. Tucci, R. Vasanthi, Heterojunction solar cell with 2% efficiency based on a Cu_2O substrate, *appl. Phys. Lett.* 88 (2006) 163502.
- [12] J. Cui, U. J. Gibson, A simple two-step electrodeposition of $\text{Cu}_2\text{O}/\text{ZnO}$ nanopillar solar cells, *J. Phys. Chem. C* 114 (2010) 6408-6412.
- [13] M. Izaki, T. Shinagawa, K. Mizuno, Y. Ida, M. Inaba, A. Tasaka, Electrochemically constructed p- $\text{Cu}_2\text{O}/\text{n-ZnO}$ heterojunction diode for photovoltaic device, *J. Phys. D* 40 (2007) 3326-3329.
- [14] M. Ichimura, Y. Song, Band alignment at the $\text{Cu}_2\text{O}/\text{ZnO}$ heterojunction, *Jpn. J. Appl. Phys.* 50 (2011) 051002.
- [15] D. L. A. de Faria, S. Venancio Silva, M. T. de Oliveira. Raman microspectroscopy of some iron oxides

and oxyhydroxides, *J. Raman Spec.* 28 (1997) 873-878.

[16] S. J. Oh, D. C. Cook, H. E. Townsend, Characterization of iron oxides commonly formed as corrosion products on steel, *Hyperfine Interactions* 112 (1998) 59-66.

[17] T. Ohtsuka, K. Kubo, N. Sato, Raman spectroscopy of thin corrosion films on iron at 100 to 150 °C in air, *Corrosion* 42 (1986) 476-481.

[18] Q. Han, Z. Liu, Y. Xu, Z. Chen, T. Wang, H. Zhang, Growth and Properties of Single-Crystalline γ -Fe₂O₃ Nanowires, *J. Phys. Chem. C* 111 (2007) 5034-5038.

Figure captions

Figure 1 Differential Auger spectra of as-deposited (a) and 400°C - annealed (b) Fe-O thin films. The indicated Fe/O ratio is estimated using Fe₂O₃ as the standard.

Figure 2 Raman spectra of (a) as-deposited and (b) annealed Fe-O thin films. Annealing temperature is indicated in (b).

Figure 3 SEM images of Fe-O thin films annealed at different temperatures: (a) 100, (b) 200, (c) 300, and (d) 400°C.

Figure 4 Optical transmission (in %) of as-deposited and annealed Fe-O thin films at different calcination temperatures: 100, 200, 300, and 400°C. Inset shows the Tauc's plot for band gap estimation of as-deposited Fe-O film as representative.

Figure 5: PEC response of as-deposited and 100°C-annealed Fe-O thin films.

Figure 6 J-V characteristics of Cu₂O/Fe-O heterostructures with (a) γ -FeOOH and (b) α -Fe₂O₃ *n*-type layers.

Figure 7 Photovoltaic characteristics of Cu₂O/Fe-O heterojunctions with as-deposited and annealed Fe-O thin films.

Table.1. Fe/O composition ratios and bandgap of the as-deposited and annealed Fe-O films.

	As-dep	100°C	200°C	300°C	400°C
Fe/O ratio	0.52	0.53	0.66	0.67	0.67
Bandgap (eV)	2.3	2.3	2.2	2.2	2.1

Table.2. Solar cell parameters of the Cu₂O/Fe-O samples under different condition.

	As-dep	100°C	200°C	300°C	400°C
V _{oc} (V)	0.093	0.064	0.108	0.066	0.038
J _{sc} (mA/cm ²)	0.93	1.15	0.74	1.58	1.12
FF	0.30	0.26	0.35	0.30	0.28
η (%)	0.026	0.019	0.027	0.028	0.011

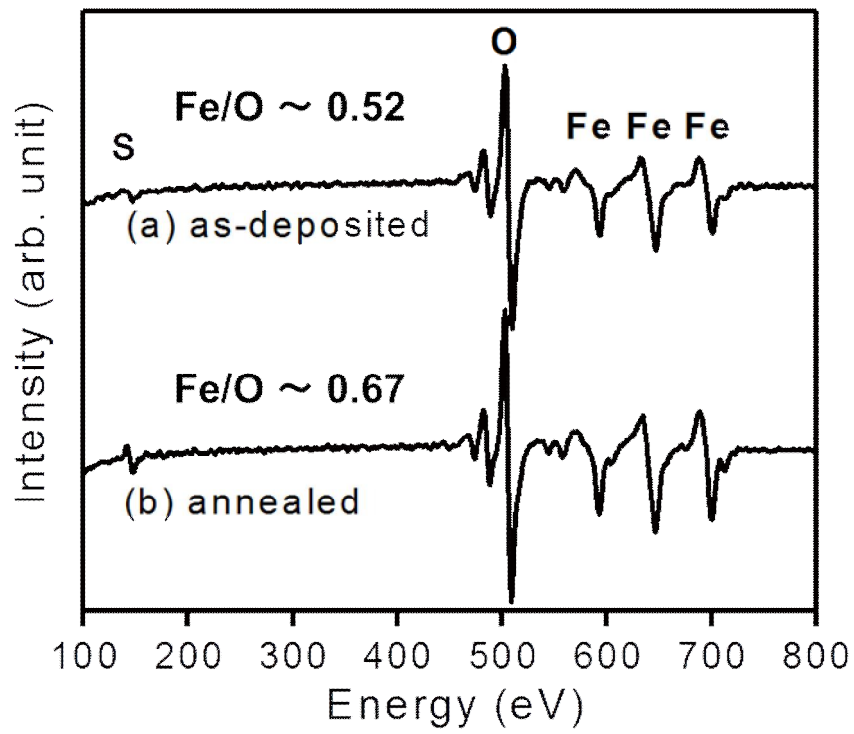


Figure 1 Differential Auger spectra of as-deposited (a) and 400°C - annealed (b) Fe-O thin films. The indicated Fe/O ratio is estimated using Fe_2O_3 as the standard.

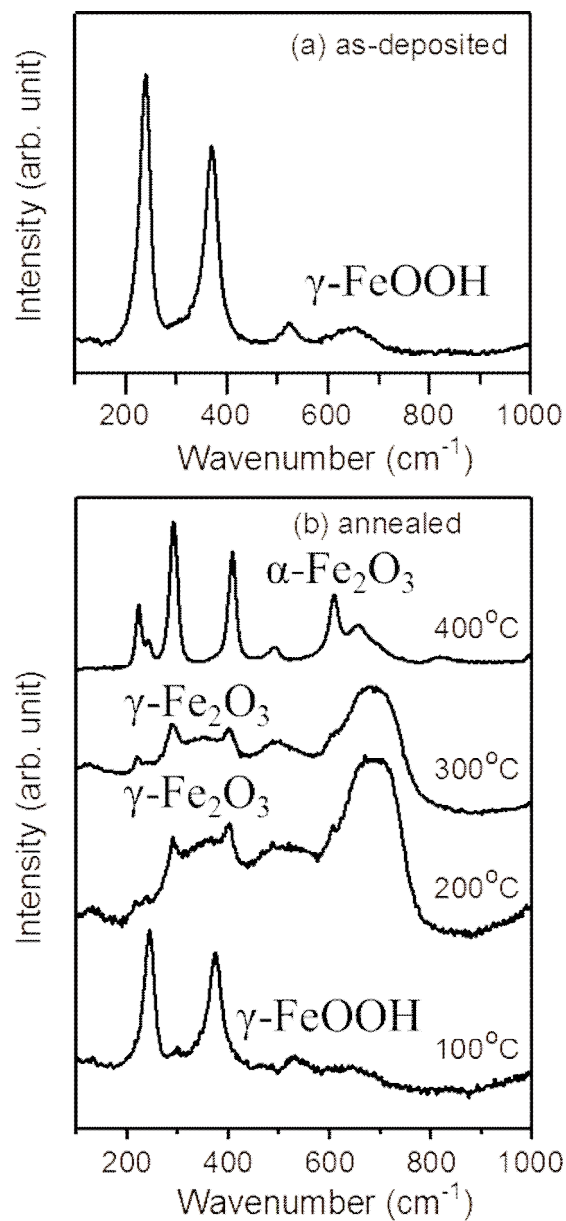


Figure 2 Raman spectra of (a) as-deposited and (b) annealed Fe-O thin films. Annealing temperature and the phases of Fe-O films are indicated in (b).

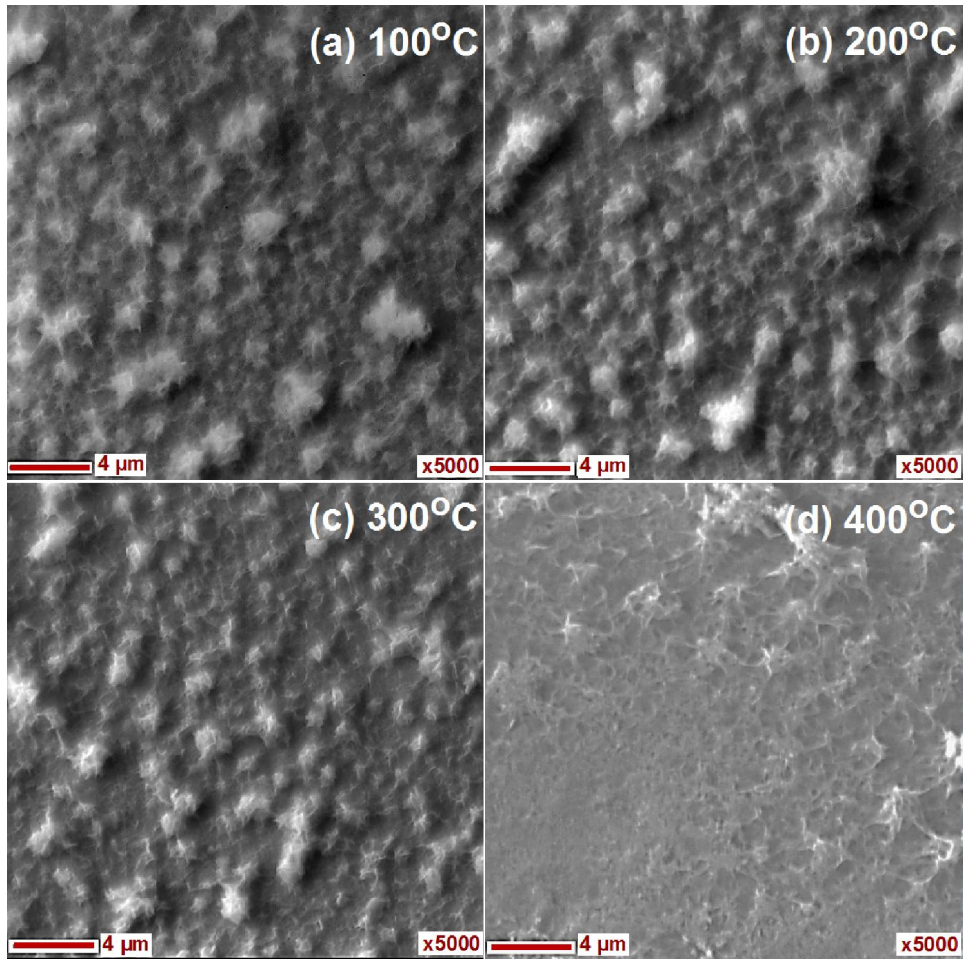


Figure 3 SEM images of Fe-O thin films annealed at different temperatures: (a) 100, (b) 200, (c) 300, and (d) 400 °C.

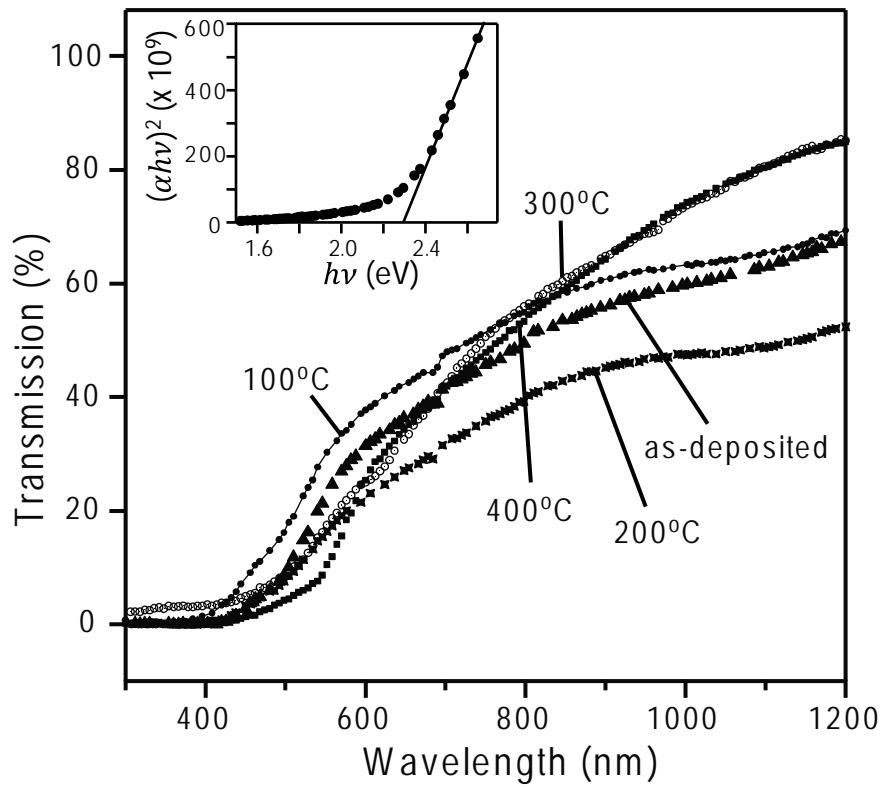


Figure 4 Optical transmission (in %) of as-deposited and annealed Fe-O thin films at different calcination temperatures: 100, 200, 300, and 400°C. Inset shows the Tauc's plot for band gap estimation of as-deposited Fe-O film as representative.

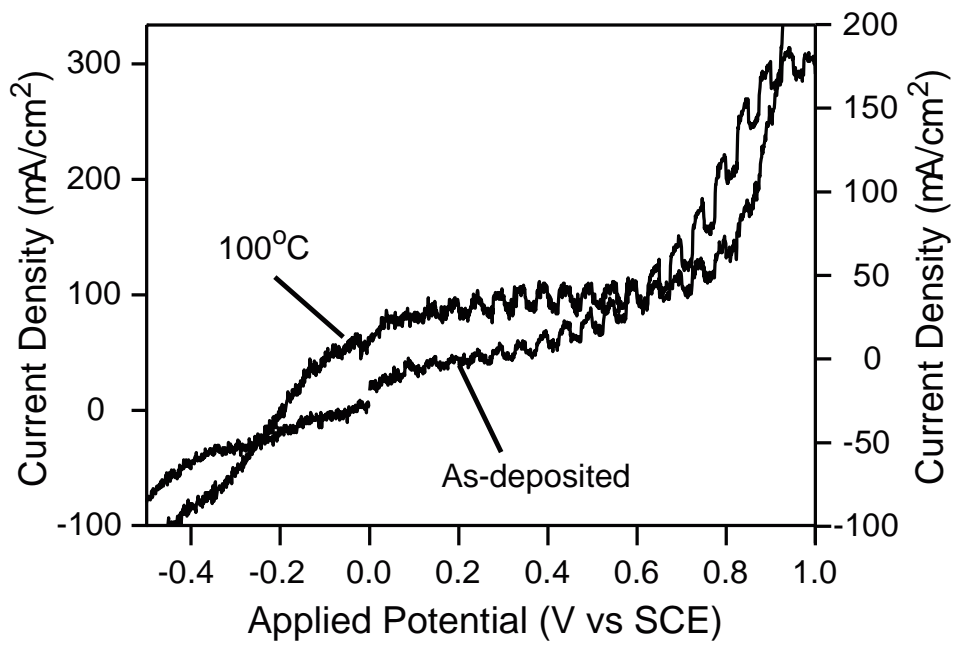


Figure 5: PEC response of as-deposited and 100°C-annealed Fe-O thin films.

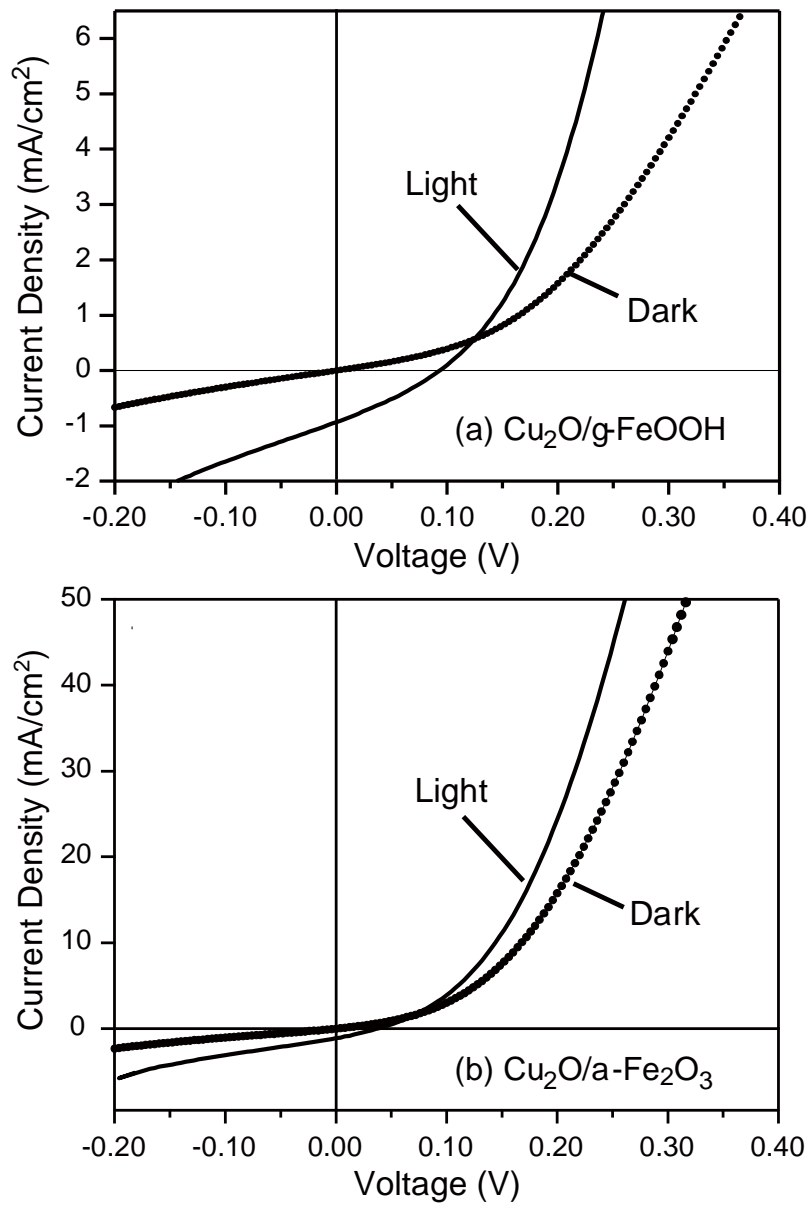


Figure 6 J-V characteristics of Cu₂O/Fe-O heterostructures with (a) γ -FeOOH and (b) α -Fe₂O₃ *n*-type layers.

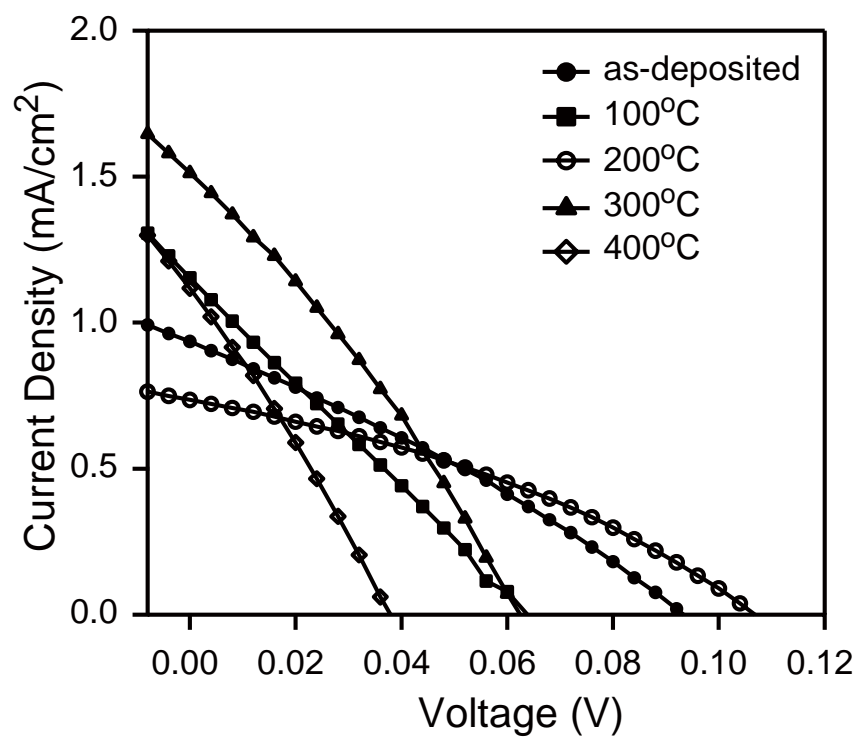


Figure 7 Photovoltaic characteristics of Cu₂O/Fe-O heterojunctions with as-deposited and annealed Fe-O thin films.